Timing, Petrogenesis, and Setting of Paleozoic Synorogenic Intrusions from the Altai Mountains, Northwest China: Implications for the Tectonic Evolution of an Accretionary Orogen

Tao Wang,[1] *Da-wei Hong, Bor-ming Jahn,*[2] *Ying Tong, Yan-bin Wang,*[1] *Bao-fu Han,*[3] *and Xiao-xia Wang*[4]

Institute of Geology, Chinese Academy of Geological Sciences, Beijing 100037, China
(e-mail: taowang@cags.net.cn)

ABSTRACT

The Altai Mountains are a key area for understanding the development of the Altai Tectonic Collage and accretionary orogen. However, the orogenic processes, particularly their early stage, have not been well understood. In this work, we undertake zircon U-Pb dating of six Paleozoic synorogenic plutons in order to better define the early magmatic and tectonic evolution of the Chinese Altai Mountains. The results revealed three Paleozoic granitic plutonic events at ca. 460, 408, and 375 Ma. These ages, along with the structural patterns of the plutons, suggest two periods of regional deformation, 460–410 Ma and 410–370 Ma. The granitoids mainly follow the tholeiitic and calc-alkaline trends and are mostly I type. Sr-Nd isotopic analyses indicate that the sources of the granitoids contain both old continental and younger (juvenile) mantle-derived components. Chemical, isotopic, and structural features suggest that the plutons were formed mainly in continental arc settings and that the subduction and accretion processes began at ca. 460 Ma and culminated at ca. 408 Ma. Thus, the Altai orogen was mainly built up during early-middle Paleozoic time, rather than during late Paleozoic time. Furthermore, the southern Altai terrane comprises not only Silurian to Devonian island arcs but also old continental fragments. With these new constraints, we present a new model to account for the tectonic evolution of the Altai orogen. This model proposes that early-middle Paleozoic Altai orogenic processes could have experienced formation of an active continental margin, the splitting of this margin to form a back-arc oceanic basin, and the final closing of the back-arc basin. Consequently, the opening and closure of back-arc basins along active margins is probably a common process in the central Asian accretionary orogen.

Online enhancements: appendixes.

Introduction

The Altaid collage of central Asia (Sengor et al. 1993), or Central Asian Orogenic Belt (CAOB; Jahn et al. 2000*a*, 2000*b*), is the world's largest and most typical Paleozoic to Mesozoic accretionary orogen. Sengor et al. (1993) proposed that the belt formed by successive accretion of a long-lived single-subduction system. Recent studies, however, revealed that the belt is a collage of various terranes or tectonostratigraphic units that include Precambrian continental blocks, and its evolution is more complicated than the single-subduction-accretion model has implied (e.g., Coleman 1989; Badarch et al. 2002; Windley et al. 2002; Xiao et al. 2004). To understand such a complicated orogen, study of all stages of development is imperative.

The Altai orogen is the key to understanding the development of accretionary orogeny in central Asia. However, its orogenic history, particularly its early stage, has not been well understood. Voluminous granitic gneisses and gneissic granitoids occur in the Chinese Altai orogen and occupy ca. 70% of the area (Windley et al. 2002). However, few stud-

Manuscript received October 28, 2005; accepted June 12, 2006

[1] Beijing SHRIMP Center, Chinese Academy of Geological Sciences, Beijing 100037, China.
[2] Institute of Earth Sciences, Academia Sinica, Taipei 115, Taiwan.
[3] Key Laboratory of Orogenic Belt and Crustal Evolution, Peking University, Beijing 100871, China.
[4] Development Research Center, Geological Survey of China, Beijing 100037, China.

[The Journal of Geology, 2006, volume 114, p. 735–751] 0022-1376/2006/11406-0006$15.00

ies (e.g., Zou et al. 1989; Zhao et al. 1993; Hu et al. 2000; Chen and Jahn 2002) have been published on the geochemistry and isotopic compositions these granitoids. Their ages have not been well constrained. Some Rb-Sr, K-Ar, and Ar-Ar ages have been published for the Altai granitoids that give a Hercynian or late Paleozoic age (e.g., He et al. 1990, 1994; Liu 1990, 1993; Zhang et al. 1996*a*, 1996*b*; Hu et al. 1997, 2000; Wang et al. 1998), but they are often contradictory or ambiguous. In this article, we present the results of zircon U-Pb dating and geochemical and isotopic analyses, and we discuss the petrogenesis and tectonic setting of the deformed granitic plutons in order to better understand the early stages of the magmatism and tectonic development of the Altai orogen. Finally, we propose a new model to explain the subduction and accretion processes in the Altai orogen.

Regional Geology

The Altai orogen is situated between the south Siberian Sayan block to the north and the Junggar block to the south (Xiao et al. 1992). It consists of several fold belts (He et al. 1990), which are also referred to as terranes (Badarch et al. 2002; Windley et al. 2002) or tectonostratigraphic units (Li et al. 2003; Xiao et al. 2004). According to Windley et al. (2002), the Altai orogen in China is composed of five terranes or units (fig. 1). We have adopted this tectonic division and use the term "units."

From north to south, unit 1 consists largely of mid-late Devonian andesite and dacite and late Devonian to early Carboniferous metasediments. The Devonian volcanics were formed in an island arc setting, and the sediments were deposited conformably on the island arcs in the associated fore-arc basin.

Units 2 and 3 constitute the central part of the Altai orogen. Unit 2 consists predominantly of Neoproterozoic (Sinian) to middle Ordovician low-grade sedimentary and volcanic rocks (the Habahe Group), with minor early Devonian sedimentary and volcanic rocks. Unit 3 contains amphibolite- and greenschist-facies metasediments and metavolcanics. Units 2 and 3 may belong to a single unit (Windley et al. 2002), and they constitute the most important part of the Altai microcontinent (Li et al. 2003; Xiao et al. 2004). In this article, we employ the term "unit 3" as the equivalent of the combination of units 2 and 3.

Unit 4 occurs in the southern Altai orogen and contains the Kangbutiebao and Altai formations (Windley et al. 2002). The Kangbutiebao formation comprises late Silurian–early Devonian volcanic and pyroclastic rocks and a small amount of basic volcanic rock. These rocks were previously considered a formation in a continental rifting setting (Han and He 1991); however, recent studies (e.g., Windley et al. 2002; Xiao et al. 2004) suggest that they formed in an arc setting. A zircon age of 407 ± 9 Ma was obtained for a felsic volcanic rock from the formation (Zhang et al. 2000). The Altai Formation is composed of low-grade metamorphic rocks that contain fossils of mid-Devonian age, and it was thought to have formed in a fore-arc basin (Windley et al. 2002). Recently, an ophiolite was found in the central part (Kuerti area) of unit 4 (fig. 1; Xu et al. 2001, 2003). A plagiogranite from the ophiolite was dated at 372 ± 19 Ma by SHRIMP zircon U-Pb analyses (Zhang et al. 2003). In addition, a suite of amphibolite-facies metasedimentary rocks occurs in unit 4, and the rocks were intruded by a granitic pluton at 462 Ma (see below).

Unit 5 is composed mainly of Devonian fossiliferous successions that are, in turn, overlain by late Carboniferous formations. Gneisses and schists also occur locally. It is separated from unit 6 (i.e., the Junggar block) by the Erqis fault (fig. 1). Unit 6 is made up principally of Devonian island arc rocks, with a small amount of Ordovician limestone and some Carboniferous island-arc volcanics (Mei et al. 1993).

The Erqis fault, one of the largest transcurrent faults in central Asia, bounds the Altai orogen to the north and the Junggar block (Kazakhstan plate) to the south (Sengor et al. 1993; He et al. 1994). The fault zone contains an ophiolite with a zircon U-Pb age of 390 Ma (Wang et al. 2003) and was considered to be the site of early to middle Paleozoic subduction (e.g., He et al. 1994; Xiao et al. 2004). During late Paleozoic (290–280 Ma) time, the zone experienced large-scale (1000 km) sinistral displacement (e.g., Laurent-Charvet et al. 2003).

Pluton Characteristics and Sample Description

The plutons in the Chinese Altai orogen can be roughly divided into two groups—deformed syntectonic (or synorogenic) and undeformed posttectonic (or postorogenic)—according to their deformation patterns and relation to the regional geology. Six syntectonic plutons are studied here, and their principal characteristics are described as follows.

Qiemuerqieke Pluton (Samples 161–169). This pluton is located in the western part of unit 4 (fig. 1), and the country rocks are amphibolite-facies

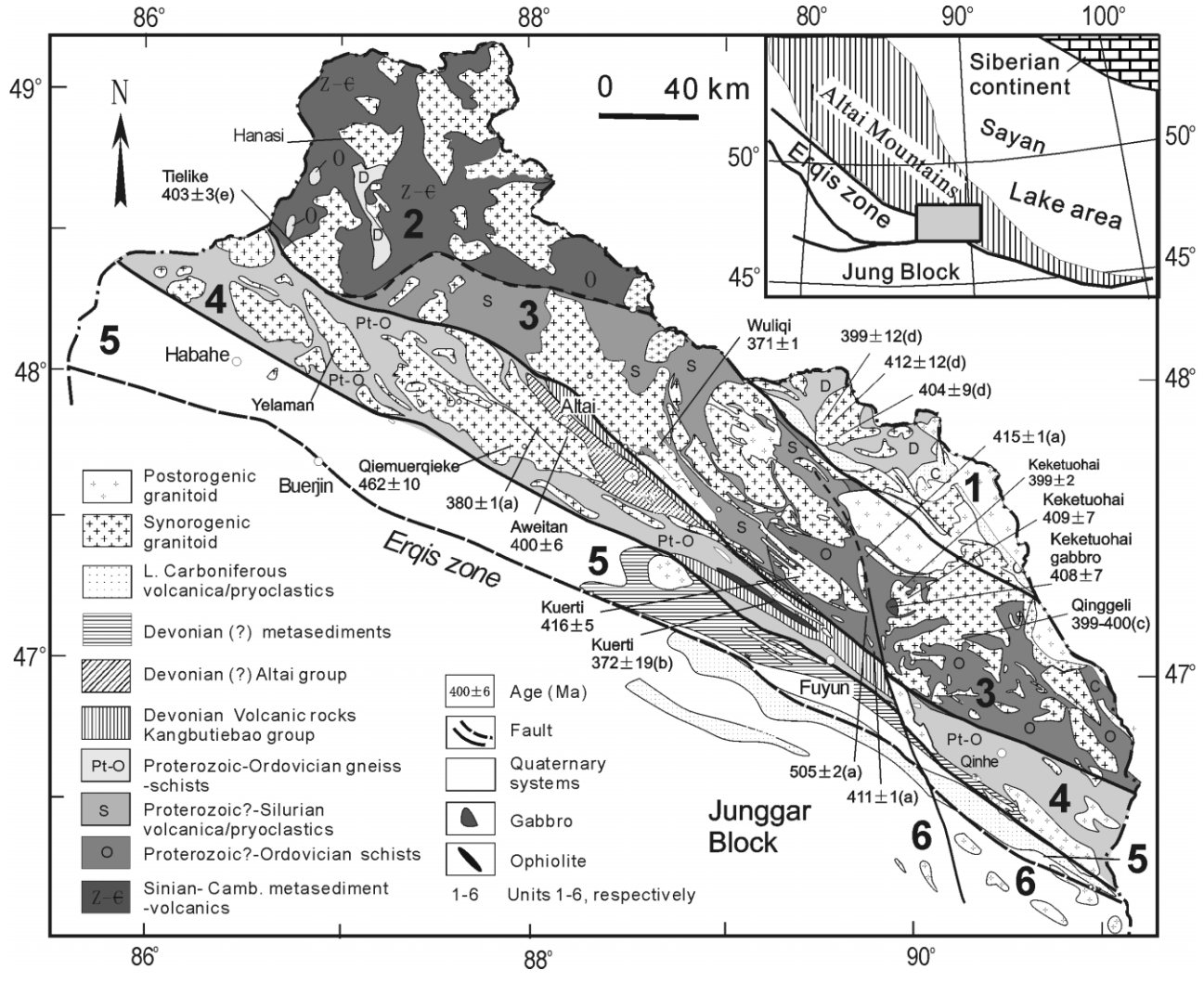

Figure 1. Generalized geological map of the Chinese Altai orogen, modified from Zou et al. (1989), Zhang et al. (2000), Windley et al. (2002), Li et al. (2003), Xiao et al. (2004), and our new data. The studied plutons are marked by their names and our zircon U-Pb ages (Ma). Other age sources: *a*, zircon Pb-Pb ages from Windley et al. (2002); *b*, zircon U-Pb SHRIMP age from Zhang et al. (2003); *c*, zircon U-Pb ages from Wang et al. (1998); *d*, zircon Pb-Pb ages from Lou (1997); *e*, zircon age from Tong et al. (2005).

gneisses. It is the largest and most strongly deformed granitic pluton in the Altai orogen. The constituent rocks are granitic gneisses with strong and pervasive foliation and mineral lineation as well as folding (fig. 2*a*). Their clear and sharp contacts with the regional metamorphic gneisses indicate they are intrusive (fig. 2*b*). The rock types of the pluton are mainly tonalitic and granodioritic. Their principal minerals include plagioclase, alkali feldspar, quartz, and biotite, with a minor amount of hornblende.

Our studied samples came from the central and eastern parts of the pluton. Sample 161/1 (fig. 2) was chosen for zircon U-Pb dating. It contains plagioclase (30%–40%), alkali feldspar (20%–30%), quartz (20%–30%), and biotite (5%–7%). Accessory minerals are zircon, apatite, ilmenite, and titanite.

Aweitan Pluton (Samples 138–141). The Aweitan pluton occurs to the northeast of the Qiemuerqieke pluton (fig. 1). The two plutons contact, though their clear relation is not observed. The Aweitan pluton shows moderate gneissic foliation. The orientation of compositional stripes and elongated feldspar and quartz are features of submagmatic flow and high temperature solid-state deformation for a syntectonic pluton (Paterson et al. 1989). The

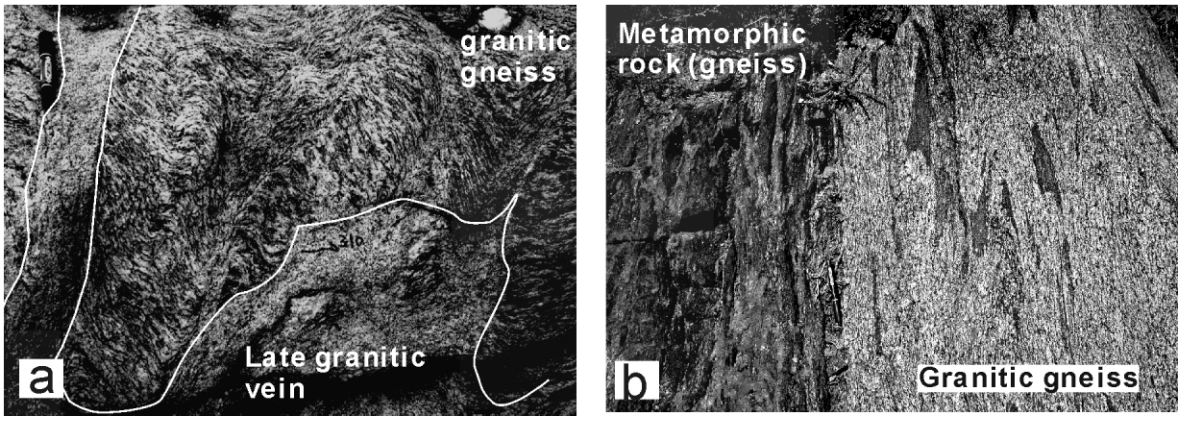

Figure 2. Field photos for the Qiemuerqieke granitoid gneiss (sample 161/1), showing strong deformation (*a*) and its contact with the country rocks (*b*). The gneissic foliation is characterized by compositional stripes (ribbons of feldspar aggregates) that show high-temperature solid-state deformation fabrics. The foliations are folded and intruded by later granitic veins, indicating a strong late tectonic event. Two pens (15 cm long) indicate scale.

pluton consists mainly of highly foliated granodiorite, intruded by weakly foliated monzogranite. Sample 138/1 was collected from an outcrop of the strongly foliated granodiorite about 2 km southeast of Altai City. It consists of plagioclase (50%–55%), alkali feldspar (10%–15%), quartz (20%–30%), biotite (5%–6%), and accessory minerals.

Keketuohai Pluton (Samples 102–131). This pluton is located in the eastern part of unit 3. It also shows foliation and lineation of different scales. The rock types include tonalite, biotite granodiorite, and biotite monzogranite. Mafic enclaves are abundant, particularly in the margin close to the Keketuohai mafic (gabbro) pluton. Sample A8 was collected from the northern part of Keketuohai Township. Sample 120/3 came from a locality about 5 km southeast of the town, on the south side of the Erqis River. Both samples are of coarse- to medium-grained granodioritic rocks that are composed of plagioclase, alkali feldspar, quartz, and biotite.

In addition, several small plutons (e.g., the Qingeli pluton) occur to the south of the Keketuohai pluton. They are composed mainly of granodiorite and diorite. The Qingeli diorite pluton has a zircon U-Pb age of 399–410 Ma (Wang et al. 1998).

Keketuohai Mafic Pluton (Samples 120/4–122/2). This gabbro-diorite pluton occurs in the west of the Keketuohai pluton (fig. 1). It is partly altered to amphibolitic rocks. Sample 122/2 was collected from the roadside about 20 m northwest of the Altai Number 3 open-pit pegmatite mine. The rock consists mainly of plagioclase (50%–60%) and blue-green hornblende (35%–45%). Some hornblende grains contain pyroxene cores.

Kuerti Pluton (Samples 3045–3051). This pluton occurs in the southern part of unit 3. It is composed mainly of biotite granodiorite and biotite monzogranite. The principal minerals comprise plagioclase, alkali feldspar, quartz, and biotite. Some rocks contain muscovite (<3%, sample 3045); others contain hornblende (2%, sample 3049). The textural characteristics, including compositional banding and preferred orientation of biotite, elongated quartz, and feldspar, are consistent with magmatic flow and high temperature solid-state deformation (Paterson et al. 1989, 1998).

Wuliqi Pluton (Samples 149–153, 9710). The pluton is located in the central part of unit 3 (fig. 1). Foliation and lineation are variably developed within the pluton. The rock types include tonalite, biotite granodiorite, and biotite monzogranite. Sample 9710 is granodiorite that was collected south of the Daqiao bridge. Its primary minerals are plagioclase, alkali feldspar, quartz, and biotite. Some small, undeformed granitic stocks (granodiorite, monzogranite) intruded the pluton; one of them was dated at 267 Ma by the zircon U-Pb SHRIMP method (our unpublished data).

Zircon U-Pb Dating Results

Zircon grains were separated from seven samples and dated by U-Pb SHRIMP and thermal ionization mass spectrometry (TIMS) methods (for details, see app. A, available in the online edition or from the *Journal of Geology* office). The zircon grains from the granitoid are colorless or light brown, transparent, and generally euhedral (tetragonal pyramid).

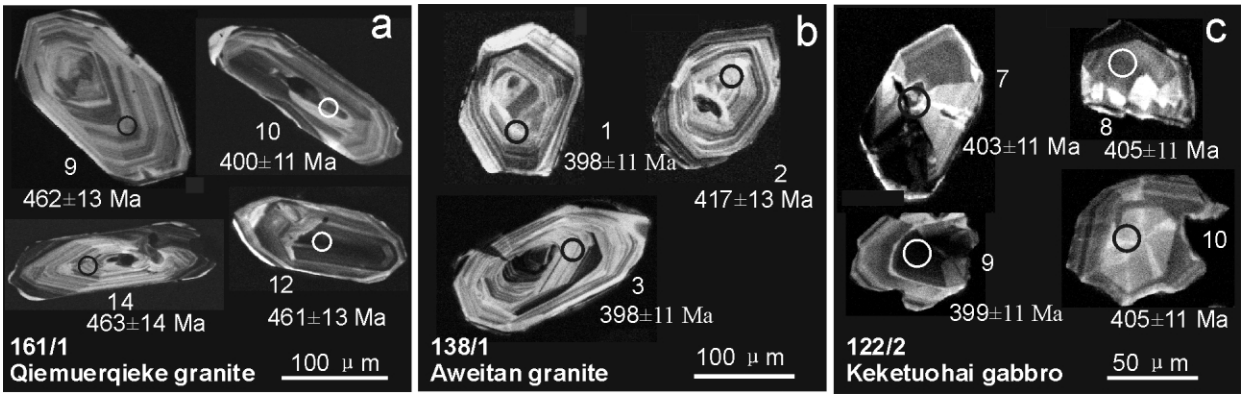

Figure 3. Cathodoluminescence images of SHRIMP-analyzed zircons of sample 161/1 from the Qiemuerqieke granitic gneisses (a), sample 138/1 from the Aweitan gneissic granites (b), and sample 120/3 from the Keketuohai mafic pluton (or Keketuohai gabbro; *c*). Analyzed spots are circled, and codes correspond to the results in table B1. Numbers are $^{206}Pb/^{238}U$ ages.

They are elongated, short prismatic, or stubby. Their sizes range from 100 to 400 μm along the long axis. Almost all grains display well-developed concentric oscillatory zoning, suggesting magmatic origin (e.g., fig. 3*a*, 3*b*). A few grains have inherited cores.

Zircon grains of the Keketuohai gabbro (sample 122/1) are small (50–150 μm). Some are irregular or spear-headed in shape (fig. 3*c*). Their internal features show fanlike and wide concentric oscillatory zoning. No inherited core is observed. These are typical of zircon grains from mafic intrusions.

Qiemuerqieke Pluton (161/1, 462 ± 10 Ma). Sixteen spots were analyzed on zircon grains of sample 161/1 (table B1, available in the online edition or from the *Journal of Geology* office). Ten data points define a population with a $^{206}Pb/^{238}U$ age of ca. 460 Ma (fig. 4). In this population, the oldest (point 7) and youngest (point 16) data points were excluded from the age calculation. The remaining eight concordant data points (1, 2, 5, 6, 9, 11, 12, 15) yielded a weighted mean $^{206}Pb/^{238}U$ age of 462 ± 10 Ma, with MSWD = 1.4, which is the same as that of the most concordant data spot 12 (461 Ma). The analyzed zircon cores have a magmatic feature (fig. 3*a*); they are not inherited cores, as are often found in metamorphic rocks. In addition, the ages of the cores (e.g., spot 12, fig. 3*a*) are almost the same as those obtained for the zircon grains without cores (e.g., spots 9, 14; fig. 3*a*).

Three data points (spots 8, 10, 14) show $^{206}Pb/^{238}U$ ages ranging from 400 to 370 Ma, but they are discordant and dispersive (fig. 4). Three other data points (spots 3, 4, 13) show much younger $^{206}Pb/^{238}U$ ages, from 372 to 335 Ma.

Aweitan Pluton (Sample 138/1, 400 ± 6 Ma). Fifteen spots were analyzed for sample 138/1 (table B1). Fourteen data points are tightly grouped, yielding a $^{206}Pb/^{238}U$ age of 400 ± 6 Ma, with MSWD = 0.56 (fig. 5*a*). The one point left (spot 10) was analyzed on a core, which we interpreted as inherited, and it gave a $^{206}Pb/^{238}U$ age of 637 Ma.

Keketuohai Mafic Pluton (Sample 122/2, 408 ± 6 Ma). Thirteen measurements were made for sam-

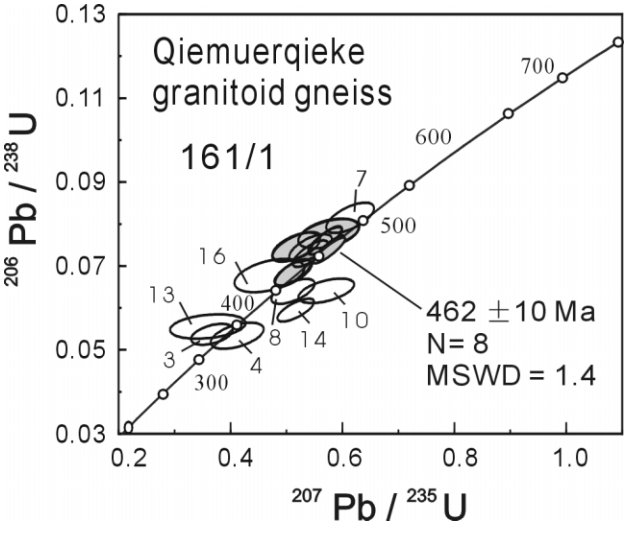

Figure 4. U-Pb concordia diagram showing zircon ages from sample 161/1 of the Qiemuerqieke pluton (granitic gneisses). Eighteen data for age calculation are marked with gray. The others that are marked by numbers are not taken into account. The data numbers correspond to those in table B1.

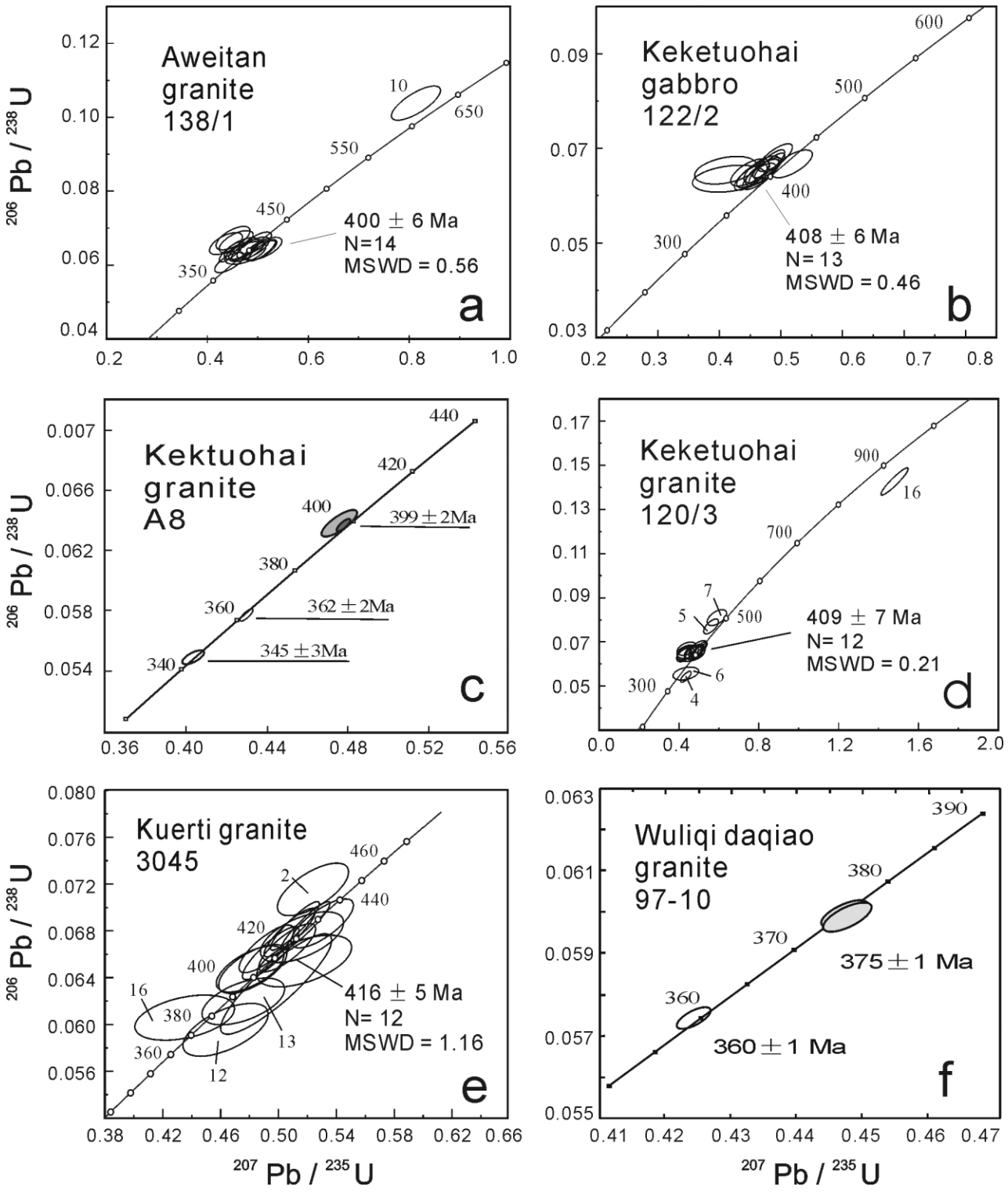

Figure 5. U-Pb concordia diagram showing zircon ages obtained by SHRIMP (*a*, *b*, *d*, *e*) and by thermal ionization mass spectrometry (*c*, *f*) of the 410–375 Ma plutons. In *d*, *e*, the data points with their numbers were not used in the age calculation. Data that are excluded from age calculation are marked by their numbers (see table B1).

ple 122/2. They are all tightly grouped and yield a $^{206}Pb/^{238}U$ age of 408 ± 6 Ma, with MSWD = 0.64 (table B1; fig. 5*b*).

Keketuohai Pluton (Sample A8, 399 ± 2 Ma; 120/3, 409 ± 7 Ma). Zircon grains from sample A8 were dated by the TIMS method (table B2, available in the online edition or from the *Journal of Geology* office). Two analyses yielded a weighted mean $^{206}Pb/^{238}U$ age of 399 ± 2 Ma (fig. 5*c*). The other two analyses yielded $^{206}Pb/^{238}U$ ages of 362 ± 2 and 345 ± 2 Ma.

The second sample (120/3) was dated by the SHRIMP method. Seventeen age data from this sample show a large range in $^{206}Pb/^{238}U$ ages from ca. 340 to 900 Ma (table B1). An age population (12 data points) yielded a $^{206}Pb/^{238}U$ age of 409 ± 7 Ma, with MSWD = 0.21 (fig. 5*d*). This age is consistent, within error limits, with the age of the TIMS analyses at 399 ± 2 Ma.

Data point 16 was obtained on a core and gave a discordant $^{206}Pb/^{238}U$ age of 859 Ma and $^{207}Pb/^{206}Pb$ age of 1076 ± 22 Ma. Two other data points (5 and 7) show $^{206}Pb/^{238}U$ ages of ca. 478–502 Ma. Additionally, two data points (4 and 6) yielded slightly discordant $^{206}Pb/^{238}U$ ages of 340–349 Ma.

Kuerti Pluton (Sample 3045, 416 ± 5 Ma). A total of 16 analyses were made on sample 3045 (table B1; fig. 5*e*). Data points 2, 12, 13, and 16 have low U and are slightly discordant; therefore, they were excluded from the age calculation. The other 12 data points are mostly concordant, yielding an age of 416 ± 5 Ma, with MSWD = 1.16 (fig. 5*e*).

Wuliqi Pluton (Sample 9710, 375 ± 1 Ma). The zircon grains were analyzed by the TIMS method (table B2). Two analyses yielded a weighted mean $^{206}Pb/^{238}U$ age of 375 ± 1 Ma (fig. 5*f*). One analysis (spot 3) gave a $^{206}Pb/^{238}U$ age of 361 ± 1 Ma, which is same as one age (362 ± 2 Ma) of sample A8 (Keketuohai pluton).

Chemical and Nd-Sr Isotopic Analyses

The analytical procedures for major and trace elements and Nd-Sr isotope compositions are given in appendix A. We discuss these features of the plutons by their names from oldest to youngest.

Major and Trace Elements. The samples from the Qiemuerqieke granitic pluton generally belong to tonalite and granodiorite, based on the classification of Streckeisen and Le Maitre (1979; fig. 6*a*). Their Na_2O/K_2O ratios are >2.0, indicating sodic granitoids. In a K_2O-SiO_2 diagram, all of the rocks except one fall in the tholeiitic field (fig. 6*b*). In an A/NK versus ACNK plot, the granitoid samples are weakly metaluminous to weakly peraluminous (tables B3–B5, available in the online edition or from the *Journal of Geology* office; fig. 6*c*). Their rare earth element (REE) patterns are characterized by moderate enrichment in light REEs (LREEs), flat heavy REEs (HREEs; fig. 7*a*), and slightly negative Eu anomalies. In primitive mantle (PM)-normalized spidergrams, most samples show pronounced negative anomalies in Ba, Sr, Nb, Ta, and Ti (fig. 7*b*).

Most Aweitan and Keketuohai samples fall in the calc-alkaline field and a few in the high-K calc-alkaline and tholeitic fields in the SiO_2-K_2O diagram (fig. 6*b*). They are weakly peraluminous (except tonalite 102/2 and an enclave, 107/2, which are metaluminous; fig. 6*c*). With respect to the REE abundances, they have enriched LREE and flat HREE patterns with small to moderate negative Eu anomalies (fig. 8*a*, 8*c*, 8*e*). For the Aweitan plutons, the early tonalite (138/1) does not show an Eu anomaly, but the younger granodiorites (138/1 and 141) show slightly negative Eu anomalies (fig. 8*a*), due probably to fractionation of plagioclase during magmatic differentiation. In the PM-normalized spidergrams (fig. 8*b*, 8*d*, 8*f*), all samples are characterized by negative anomalies in Ba, P, Nb, Ta, and Ti, and pronounced enrichment in Rb and Th.

The granitoids from the Kuerti pluton follow a tholeiitic trend (fig. 6*b*) and show high Na_2O/K_2O ratios (2.5–5). They are similar to those of the Qiemuerqieke pluton. Their REE patterns show moderate enrichment in LREEs and flat to depleted HREE patterns (fig. 8*e*). They show positive (sample 3047) to highly negative Eu anomalies. Sample 3045 is an exception; it has a low REE abundance pattern with a huge negative Eu anomaly. Moreover, the high K/Ba (270) and low Nd/Ta (12) and Zr/Hf (16) point to the possibility of a lanthanide tetrad affect (e.g., Bau 1996; Irben 1999; Jahn et al. 2001, 2004; Wu et al. 2004).

Samples from the Keketuohai mafic pluton have low SiO_2 (ca. 43%–46%) and moderate MgO (6.2%–9.3%) contents (table B3). They belong to tholeiitic basalt in a triangle diagram of FeO-(Na_2O + K_2O)-MgO (not shown). The REE patterns of the gabbros (122/2 and 120/4) have a slight negative slope with pronounced positive Eu anomalies (fig. 8*g*). Sample 120/5, however, shows a flat pattern without Eu anomalies (fig. 8*g*). A striking feature is that they are enriched in Sr, Rb, and K and depleted in Ba, Th, Y, and some high-field-strength elements (e.g., Nb, Ta, and Zr; fig. 8*h*).

The Wuliqi granitic pluton is lithologically and chemically similar to the plutons of ca. 408 Ma (figs. 6, 8, 9). In trace elements, two samples (151/1 and 152/2) show enriched LREEs with pro-

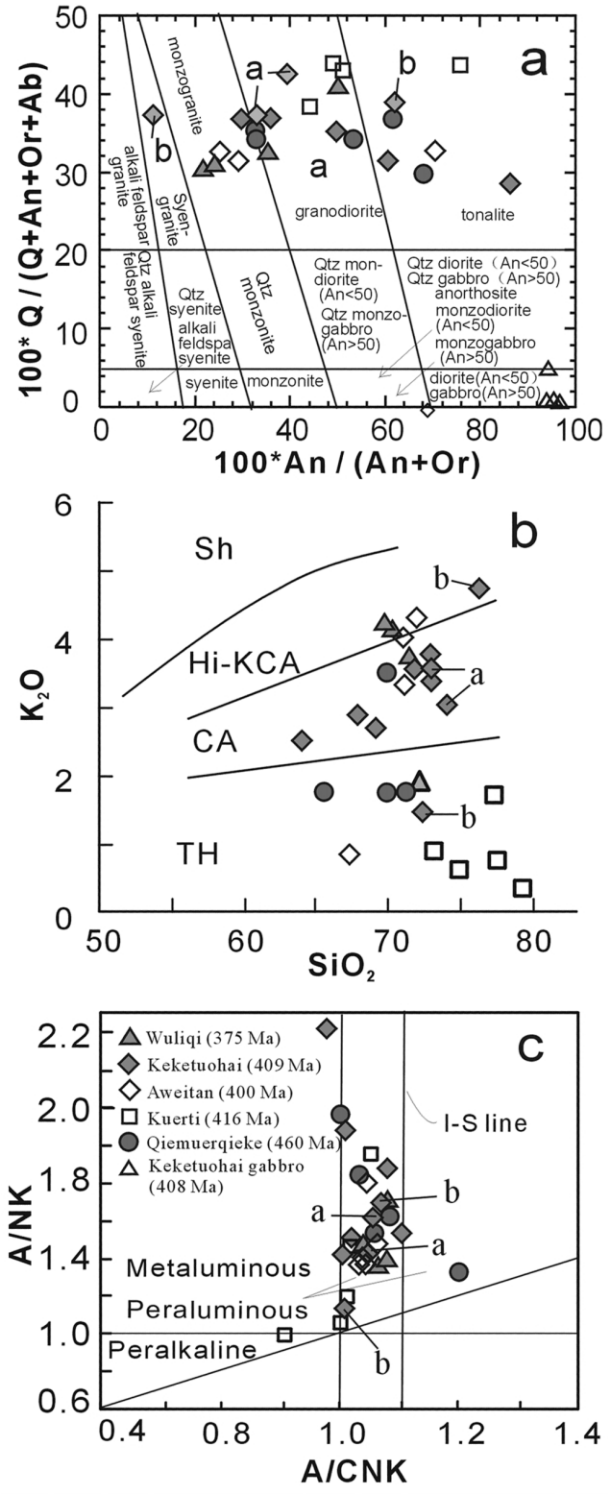

Figure 6. Major element diagrams for rock types of the synorogenic granitoids from the Chinese Altai. *a*, Q′ versus the ANOR classification scheme of Streckeisen and Le Maitre (1979); *b*, SiO_2 versus K_2O diagram (boundary after Peccerillo and Taylor 1976); *c*, A/CNK versus A/NK diagram (Shand's molar parameters in the diagram of Maniar and Piccoli [1989]), A/CNK = molar $Al_2O_3/(Na_2O + K_2O + CaO)$, A/NK = molar $Al_2O/(Na_2O + K_2O)$. SH = shoshonitic; Hi-KCA = high-K calc-alkaline; CA = calc-alkaline. Symbols in *a* and *b* are the same as in *c*. Data for *a* and *b* are from Chen and Jahn (2002) and Zhao et al. (1993).

nounced negative Eu anomalies (fig. 9*a*), and one sample (149/3) shows enriched LREEs without Eu anomalies. Another sample (149/2, granitoid gneiss) has a positive Eu anomaly. This rock may belong to the early phase of the pluton or another pluton. All the samples exhibit negative Ba, Sr, Nb, Eu, and Ti anomalies and positive Rb, Th, K, La, and Nd anomalies (fig. 9*b*).

Isotopic Compositions. Nd-Sr isotope data for 13 samples are summarized in table B6, available in the online edition or from the *Journal of Geology* office, and plotted in figure 10. The age-corrected initial Sr isotope ratios (I_{Sr}) appear to be quite variable, from <0.700 to 0.715. Most granitoids have undergone deformation and metamorphism to variable degrees, so the measured Rb/Sr and $^{87}Sr/^{86}Sr$ ratios could have been modified to some extent. Consequently, these I_{Sr} values do not provide a significant petrogenetic constraint. On the other hand, Nd isotope data are known to be more robust, and Sm/Nd ratios can be more accurately measured, relative to Sr, and they provide a much clearer and less ambiguous constraint on the origin of granitic rocks (Jahn et al. 2000*a*). The following discussion is based mainly on the Nd isotopic data. The $\varepsilon Nd(T)$ values of the samples are mostly near zero to slightly negative; only two samples show +3.8 and +2.8. Since the $f_{Sm/Nd}$ values are mainly between −0.22 and −0.46 (except two samples with −0.04 and −0.1; table B3), these granitoids give meaningful model ages (T_{DM}) from 1.6 to 0.8 Ga. The gabbros and diorites show positive $\varepsilon Nd(T)$ values of +0.2 to +2.1.

Discussion

Age Interpretation and Timing of Magmatic Events. For the Qiemuerqieke pluton, we interpret 462 ± 10 Ma as the crystallization age of the zircon, as well as the intrusion age of the pluton. The main reasons are (1) it is represented by the most concordant dates (eight points), (2) the data are obtained for all kinds of zircon and domains (such as for the zircon grains without cores) and are repre-

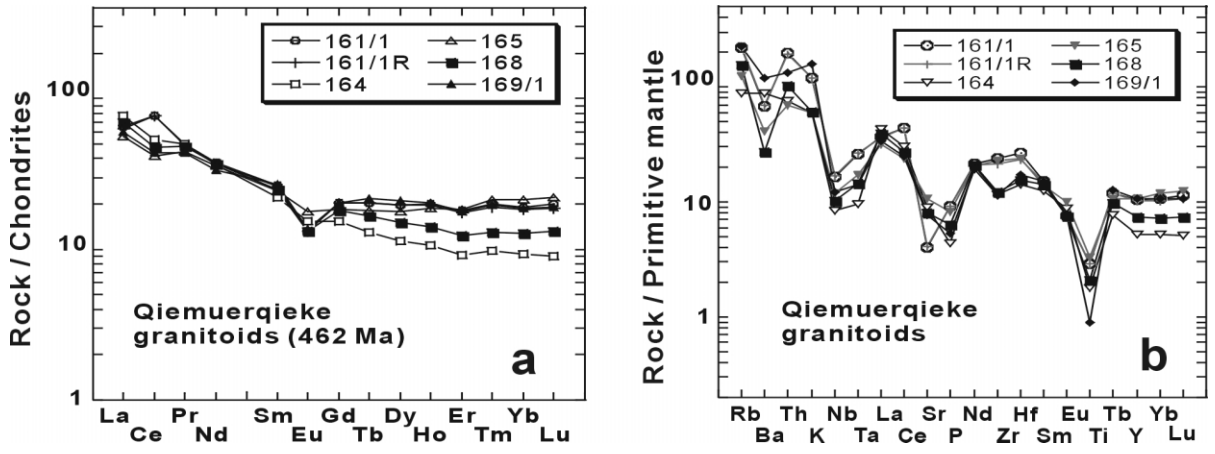

Figure 7. Rare earth element patterns (*a*) and spidergrams (*b*) of the Qiemuerqieke granitic gneisses (462 Ma) from the Altai orogen. The chondrite values and values of primitive mantle are from Sun and McDonough (1989).

sentative of these zircon grains, and (3) the structural feature (granitic gneiss) and the field relations suggest that the gneissic pluton is the oldest in the region. As for the three younger $^{206}Pb/^{238}U$ dates of ca. 400 Ma, they are discordant, and their geological signature is not clear. They could be a result of Pb loss events of older zircons. Three other much younger concordant dates (e.g., ca. 330 Ma) could reflect a late tectonothermal event. For example, there are many small granitic veins that intruded the Qiemuerqieke plutons in the sample location.

The four SHRIMP ages (400 ± 6, 416 ± 5, 409 ± 7, and 408 ± 6 Ma) of the Aweitan, Kuerti, and Keketuohai granitic plutons and the Keketuohai mafic pluton and one TIMS age (399 ± 2 Ma) of the Keketuohai pluton are identical within the error limits. All of these ages are represented by the most concordant dates and the dates obtained from various zircon domains. Therefore, we conclude that these ages represent the crystallization ages of the zircons, as well as the intrusion ages of the plutons. For the Wuliqi pluton, we choose the 375 ± 1 Ma given by two analyses (fig. 5*f*) as the zircon crystallization age and the time of the pluton emplacement. The single date of 361 ± 1 Ma of the pluton and a few younger dates (360–330 Ma) of the Keketuohai pluton could reflect late tectonothermal events, as indicated by late small granitic intrusions in the Qiemuerqieke plutons (e.g., fig. 2).

A few dates obtained from the cores of zircons give much older $^{206}Pb/^{238}U$ ages (e.g., 637 Ma for the Aweitan pluton) and $^{207}Pb/^{206}Pb$ ages (e.g., 1076 ± 22 Ma for the Keketuohai pluton). These cores are interpreted as inherited. It is not clear whether these dates are geologically meaningful. They provide information that rocks with zircon grains of Precambrian age exist in the Altai orogen. Other old age data (e.g., 478–502 Ma, fig. 5*d*) could be interpreted as inherited zircon ages from older rocks (granitoids) or mixing ages between the inherited cores and magmatic domains.

The above zircon U-Pb data reveal three major Paleozoic magmatic events (ca. 462, ca. 408, and 375 Ma) in the Altai orogen. The 462 ± 11-Ma age of the Qiemuerqieke granitic gneiss pluton qualifies it as the oldest intrusion in the region. The four new ages (400 ± 6, 416 ± 5, 409 ± 7, and 408 ± 6 Ma) of the Aweitan, Kuerti, and Keketuohai granitic plutons and the Keketuohai mafic pluton, along with similar zircon U-Pb ages of 402–386 Ma for the Qinggeli diorite pluton in the eastern Altai (Wang et al. 1998) and the 409 ± 5-Ma age reported for the Tielike pluton in the western Altai orogen (Tong et al. 2005; fig. 1), indicate that the magmatism at ca. 408 Ma was widespread and that the felsic, intermediate, and mafic intrusions were contemporaneous.

Windley et al. (2002) reported a zircon Pb-Pb evaporation age of 380 ± 1 Ma for a foliated granite adjacent to the Aweitan pluton. Moreover, a granite near Keketuohai, which probably belongs to the Keketuohai pluton, yielded a zircon SHRIMP age of 387 ± 6 Ma (S. M. Wilde, unpublished data; quoted by Chen and Jahn 2002). These ages of 380–390 Ma may reflect the late phase of the ca.-408-Ma magmatism or an independent younger granitic magmatism.

Petrogenesis and Tectonic Setting of the Magmatism: Ordovician Intrusion (462 Ma). The mineral association (e.g., hornblende) suggests that the Qie-

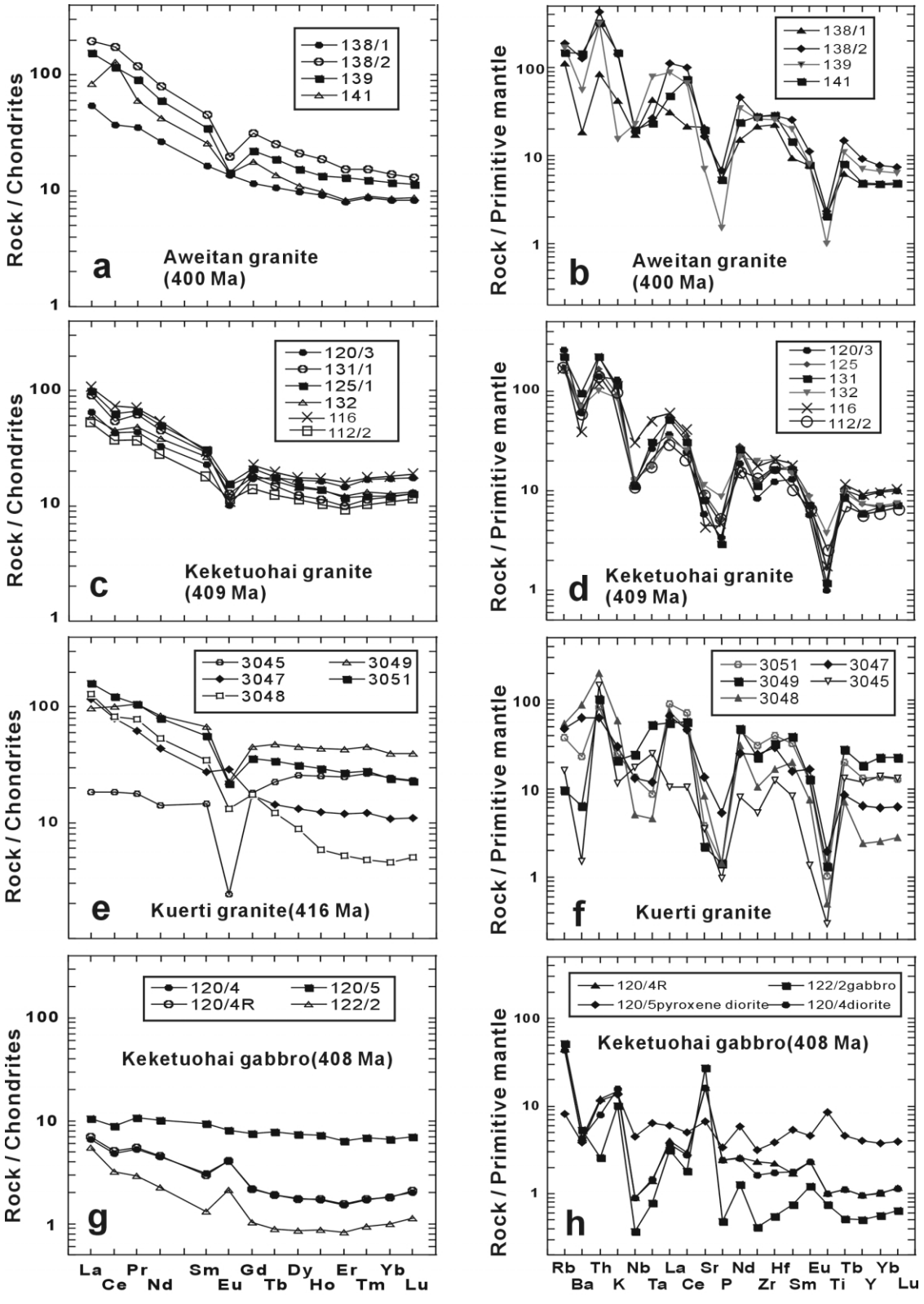

Figure 8. Rare earth element patterns (*a*, *c*, *e*, and *g*) and spidergrams (*b*, *d*, *f*, and *h*) of the intrusions with age of ca. 410–370 Ma.

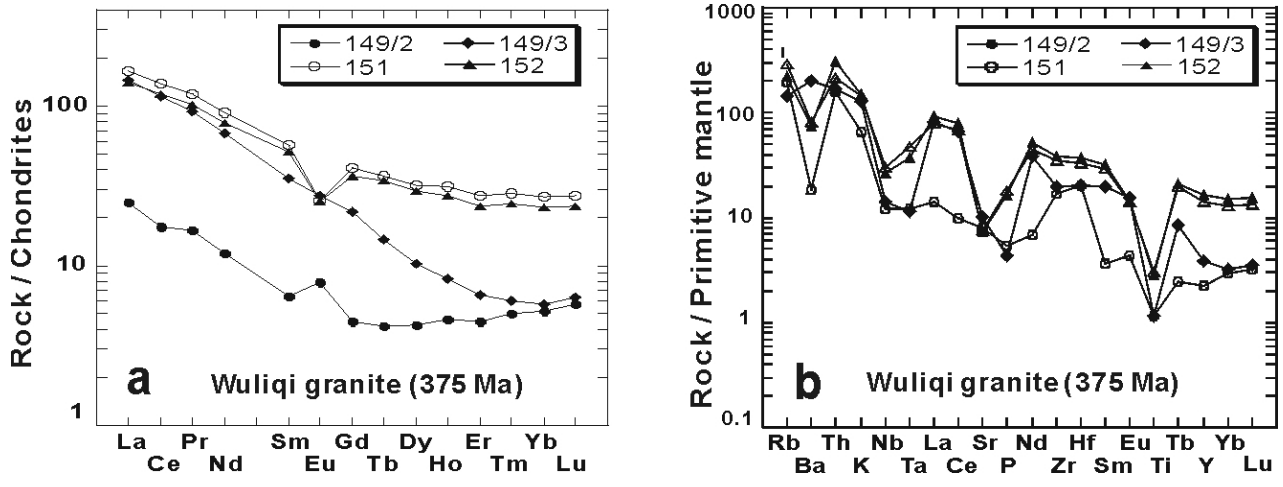

Figure 9. Rare earth element patterns (*a*) and spidergrams (*b*) of the Wuliqi granites (375 Ma).

muerqieke granites are I type, and their geochemical analyses show sodic and tholeiitic features (fig. 6*b*). Their high Th/Ta ratios (15–20, except 8.6 for sample 165) indicate subduction zone magmas (Rogers and Hawkesworth 1989), and their negative P, Nb, and Ti anomalies are also shared by arc granites (e.g., Sajona et al. 1996). In tectonic-discriminating diagrams (e.g., Ta vs. Yb and Rb vs. [Y + Nb] diagrams, not shown here), most samples fall in volcanic arc fields or in a superposed area between volcanic arc and postcollisional fields. Furthermore, the negative Ba, P, Nb, Ta, Ti, and particularly Sr anomalies and pronounced positive Rb, Th, K, and La anomalies can also be explained by an involvement of crustal melts. The high I_{Sr} (0.7062–0.7121), though not so precisely determined, and low εNd (T) values (0 to −1.2; fig. 10) also suggest that crustal materials have contributed to the granitoids. We conclude that the overall geochemical and isotopic features, along with the strong synemplacement deformation, are in favor of the Qiemuerqieke pluton having been emplaced in a continental arc setting.

Early Devonian Intrusions (ca. 408 Ma). The early Devonian granitic intrusions have calc-alkaline geochemical characteristics (fig. 6*c*). Chappell and White (1992) argued that the variation of P_2O_5 versus SiO_2 could serve as a very effective means for distinction of I- from S-type granites. In figure 11, the early Devonian granitoids seem to follow the I-type trend; hence, they are considered to be I-type granites, which is also strongly supported by the hornblende present in the Kuerti samples. Some samples (e.g., Aweitan tonalite, 138/1) have low total REEs and low $(La/Yb)_N$ ratios (3.6–9.0) and show no Eu anomalies. This is also a feature generally found only in I-type granites. In tectonic-discriminating diagrams (e.g., Ta vs. Yb, and Rb vs. [Yb + Ta] diagrams, not shown), most samples fall in volcanic arc fields. Furthermore, their negative anomalies in Ba, Sr, P, Nb, Ta, and Ti and positive anomalies in Rb, Th, K, and La are features of crustal melts. In fact, the εNd (T) values (mostly near zero) indicate a crust component in their source rocks. As a whole, the Devonian granitoids were probably formed in a continental arc setting.

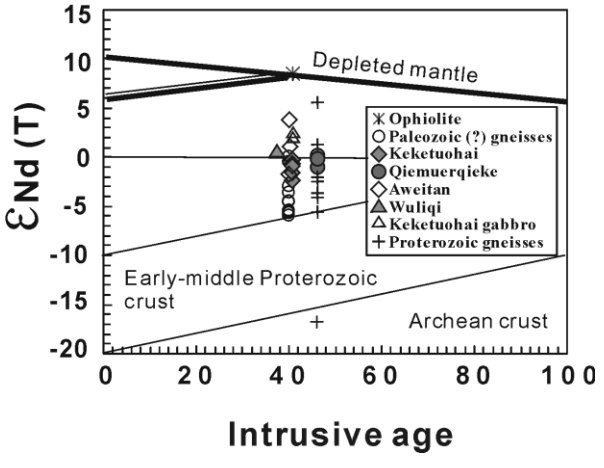

Figure 10. The ε_{Nd} (T) versus initial Sr isotope ratio diagram for intrusions from the Chinese Altai. The data for the Proterozoic and Paleozoic gneisses are from Hu et al. (2000) and Chen and Jahn (2002). The data for the ophiolite are from Xu et al. (2003).

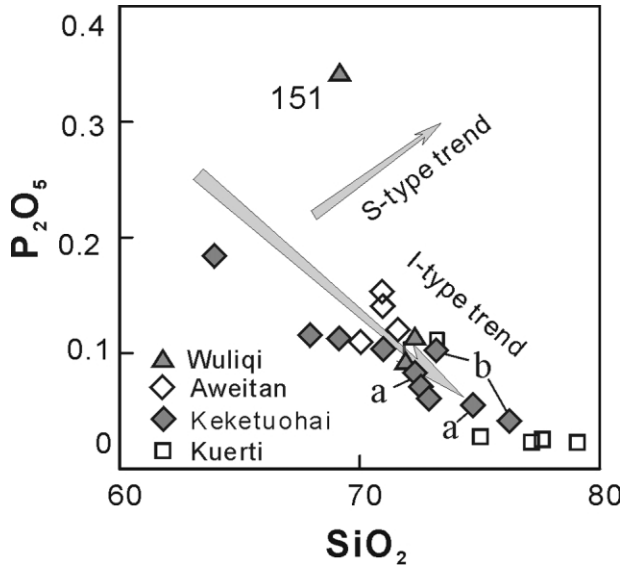

Figure 11. P_2O_5 versus SiO_2 diagram for granitoids at ca. 408 Ma, showing the variation of P_2O_5 as a function of SiO_2 content for I- and S-type granites (Chappell and White 1992).

The gabbros and diorites show εNd(T) values (+0.2 to +2.1) that are lower than the contemporary deplete mantle reservoir in the region, as represented by the gabbros (εNd [400] = +8, recalculated using data of Xu et al. 2003) of the Kuerti ophiolite, and by the 280-Ma gabbros (εNd [400] = +7.6, from our unpublished data) near Altai City. This implies that the mafic magma could have been contaminated by old continental rocks or mixed with crustally derived granitic magma. The possibility of magma mixing is supported by these petrological features: (1) mafic enclaves with igneous texture frequently occur in the granitic pluton, and they increase progressively in more mafic host rocks; and (2) mixing textures are observed, for example, quartz phenocryst rimmed by hornblende and similar mineral assemblages in both the enclaves and host rocks. Besides, the similar εNd (T) values of the mafic, intermediate, and felsic rocks are also indicative of their isotopic homogenization during magma mixing (Elberg 1996).

Late Devonian Intrusions (ca. 375 Ma). The Wuliqi granitic pluton (375 Ma) has geochemical and isotopic features similar to the granitoids of ca. 400 Ma (figs. 6, 10). They could have been derived from similar crustal sources, but the Wuliqi pluton was emplaced in the late stage of the continental arc development.

Isotopic Evidence for Continental Arc Magmatism. The isotopic features (e.g., near-zero εNd (T) values) of the granitoids in the central Altai orogen (units 2 and 3) are slightly different from those of most granitoids with high positive εNd (T) values in the CAOB (e.g., Jahn et al. 2000*a*, 2000*b*) but quite similar to those of the granitoids within or surrounding the Precambrian basement blocks or microcontinents in the CAOB, such as within the basement block in central Mongolia (Jahn et al. 2004; Kovalenko et al. 2004), within the southern Mongolia microcontinent on the China-Mongolia border (Wang et al. 2004), and within the Jiamusi block in northeast China (Wu et al. 2000). These provide evidence for the existence of the Altai microcontinent (e.g., Hu et al. 2000; Windley et al. 2002; Li et al. 2003) and for the continental arc settings for the subduction-related synorogenic granitoids. In addition, the Nd isotopic characteristics of the Altai granitoids (fig. 10) indicate that the source rocks are quite varied. They include a mantle-derived component, such as gabbro and andesite, in order to account for positive εNd (T) values, and a crustal component, such as Precambrian basement rocks, for negative εNd (T) values. Consequently, a continental arc setting best suits the magmatic evolution of the Altai orogen. The juvenile component appears most likely to be newly underplated juvenile magma(s) in a subduction setting, a proposal that is supported by the occurrence of the coeval mafic intrusions (ca. 400 Ma).

Assuming the Precambrian basement rocks with the lowest εNd (400) value (−17) and Nd = 36 ppm (Hu et al. 2000) as the crustal component end member and the depleted mantle (εNd [400] = +8, Nd = 15 ppm) as the juvenile component end member (e.g., Jahn et al. 2000*a*, 2000*b*), which happens to have the same isotopic characteristics as the middle Paleozoic Kuerti ophiolite (Xu et al. 2003), a simple mixing calculation indicates that the proportion of the mantle-derived component in the generation of the granitoids varies from 70% to 90%, a figure that constrains the maximum juvenile proportions. If the regional Paleozoic metamorphic rocks are taken as the crustal proportion (εNd [400] = −5, Nd = 25 ppm; Chen and Jahn 2002), the juvenile proportion will decrease to ca. 30%–60%, which constrains the minimum juvenile proportions. The juvenile proportions for most granitoids probably range from 60% to 70%.

Constraint on Timing of Paleozoic Regional Deformation and Accretion. As described in "Pluton Characteristics and Sample Description," the granitic plutons have typical syntectonic deformation features. For example, the foliation of the Qiemuerqieke is characterized by the orientation of (1) enclaves and compositional stripes, (2) light (rich

in quartz and feldspar) and dark (rich in biotite) banding, and (3) recrystallization aggregates of plagioclase and K-feldspar (fig. 2). These features suggest that the development of the foliation probably included magmatic flow (for 1), submagmatic flow with deformation/metamorphic differentiation (for 1 and 2), and high-temperature solid-state flow (for 3; at least >600°C; Paterson et al. 1989; 1998), all of which indicates a synemplacement deformation (i.e., the deformation could occur during and shortly after their emplacement; Paterson et al. 1989; Miller and Paterson 1994). In addition, localized ductile shear zones have never been found in the country rocks near any of these plutons. This suggests that this pluton deformation is not local but regional; thus, the deformed plutons can be viewed as regional deformation markers.

The deformation pattern of the Qiemuerqieke pluton in unit 4 indicates that regional deformation/metamorphism took place during or shortly after its emplacement (462 Ma). The Aweitan pluton (400 Ma) intruded it and shows a weaker deformation pattern. This suggests that unit 4 has undergone at least two stages of deformation: during 462–400 Ma and after 400 Ma. Similarly, in the eastern part of unit 3, an orthogneiss with a zircon Pb-Pb evaporation age of 415 ± 1 Ma (Windley et al. 2002, fig. 1) is strongly deformed. It was intruded by the Keketuohai pluton (409 ± 7 Ma), which shows a much weaker deformation pattern. This indicates that a strong regional deformation took place during 415–409 Ma in the area. Besides, the synemplacement deformation of the plutons of ca. 400 and 375 Ma in units 3 and 4 implies that the regional deformation still occurred during and shortly after their emplacement.

For the ca.-408-Ma plutons, the ones in the southern Altai orogen (unit 4; e.g., the Aweitan pluton) appear to be more strongly deformed than those (e.g., Keketuohai and Qinggeli plutons) in the central Altai orogen (unit 3). Moreover, within unit 3, southern margin plutons (e.g., the Kuerti pluton) exhibit stronger deformation in those in the northern and central part (e.g., the Keketuohai pluton; fig. 1). Therefore, the regional deformation during this time was progressively stronger from north to south. Such deformation patterns support the N-directed subduction and S-directed accretion along the southern Altai orogen.

Tectonic Evolution of the Altai Orogen: A New Model

To interpret the long-lasting synorogenic granitic activities and the tectonic evolution of the Altai orogen, the following key points from this study must be taken into consideration. (1) According to a zircon Pb-Pb age for a felsic lava, Windley et al. (2002) suggested that a continental arc was built on the southern margin of the central Altai terrane (unit 3) at ca. 500 Ma. Our age study further indicates that continental arcs still formed at ca. 460 and 416–375 Ma. Besides, the intense magmatism and deformation began at ca. 460 Ma or earlier (500–462 Ma) and culminated at ca. 408 Ma. Thus, the Chinese Altai is an early-middle Paleozoic orogen, rather than a late Paleozoic orogen. (2) The granitic magmatism at ca. 408 Ma was widespread and has geochemical characteristics of a continental arc. (3) The southern Altai (unit 4) is a key to understanding the evolution of the Altai orogen. It was considered a Silurian-Devonian island arc (Windley et al. 2002; Xiao et al. 2004; zircon age of 407 Ma, Zhang et al. 2003). However, the 462-Ma Qiemuerqieke pluton intruded the high-grade metamorphic gneisses in the southwestern part of this unit. Therefore, this part must be older than Silurian. Furthermore, the negative εNd (T) values (−1.2 to +0.5) and old Nd model ages (1.19–1.29 Ga) of the pluton, similar to those of the plutons in the central Altai (microcontinent), and the 637-Ma age of an inherited zircon from the Aweitan pluton, suggest that this part is an old continent fragment. Consequently, unit 4 should be subdivided into two units: a younger part (the island arc and ophiolite) and an older continental fragment. (4) The identification of old continental rocks from unit 4 indicates that continental fragments were involved in the early accretionary process. With these new constraints, we now propose a tectonic model, as illustrated in figure 12.

*Figure 12*a. During the early-middle Ordovician (500–460 Ma), the Paleo-Asia ocean (or the Erqis ocean here) could have been subducted northward beneath the original Altai microcontinent, forming arc volcanic rocks ca. 500 Ma, as Windley et al. (2002) suggested. The southern margin was about to be detached by back-arc extension.

*Figure 12*b. During ca. 460–410 Ma, a continental arc (the Qiemuerqieke granitic pluton) developed along the continental fragment (original unit 4), which was separated from the Altai microcontinent. A back-arc ocean, represented by the early Kuerti ocean, could also have started to form, and some (late Silurian–early Devonian?) volcanic rocks probably developed in an extensional setting (e.g., Han and He 1991). Here, we would like to emphasize that the plagioclase granite of the Kuerti ophiolite could have been derived by differentiation of mafic magma of the ophiolite or by remelting of

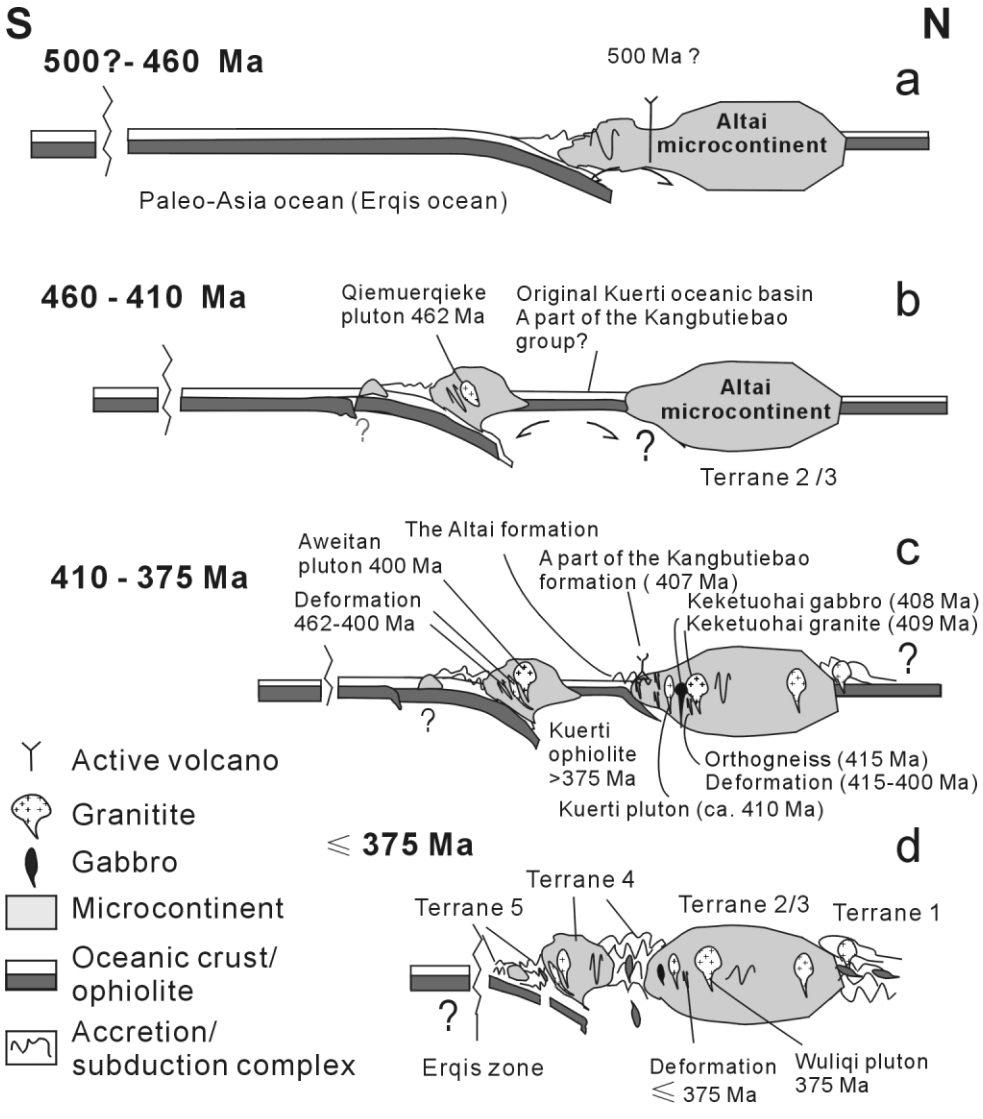

Figure 12. A tectonic model for early-middle Paleozoic subduction-accretion orogeny in the Altai orogen.

the mafic rocks of the ophiolite. In any case, the 375-Ma date of the plagioclase granite (Zhang et al. 2003) is later than the real time of emplacement, particularly the initiation of the ophiolite. Therefore, based on the regional geology, we deduce that the initiation of the ocean basin formation could have been much earlier (during the middle Paleozoic?).

*Figure 12*c. During the period from 410 to 400 Ma, the magmatism and orogeny culminated. Voluminous granitoids and volcanic rocks formed in the two microcontinental margins. Deformation of these plutons also took place during this time.

*Figure 12*d. At ca. 375 Ma, a small number of granites (e.g., the Wuliqi granites) were formed by intercrustal melting in the late stage of the continental arc (or a syncollisional setting?). Subsequently, all the tectonic units were accreted on the Altai microcontinent. Obviously, the Altai orogen is an early-middle Paleozoic orogen rather than a late Paleozoic orogen.

Generally, successive accretion is emphasized as a major process in the formation of the CAOB or Altaid collage (e.g., Coleman 1989; Sengor et al. 1993; Badarch et al. 2002; Windley et al. 2002; Xiao et al. 2004). However, the Altai orogenic process was not a simple southward successive accretion; it involved a series of processes including formation of an active continental margin, splitting of the margin to form a back-arc ocean, and the final clos-

ing of the back-arc ocean. Such a tectonic scenario is probably very common in other accretionary orogens.

Conclusions

Previous studies suggested that magmatism, regional metamorphism, and deformation in the Chinese Altai took place mainly after 360 Ma, and the area was considered to be a late Paleozoic (or Hercynian) orogenic belt. However, our study of geochemical characteristics, emplacement ages, and deformation patterns of the Altai granitic plutons suggests that the plutons were mainly emplaced in arc settings during 460–370 Ma and the strong regional ductile deformation started at least at 460 Ma and culminated at ca. 410 Ma. Consequently, the subduction and accretion processes were early to middle Paleozoic events, and the Altai orogen was mainly built up during this time but not in the Late Paleozoic. Our study also suggests that opening and closure of backarc basins along active continental margins, in addition to a successive forearc accretion, are probably common processes in the formation of the typical central Asian accretionary orogenic systems and of other accretionary orogens.

ACKNOWLEDGMENTS

S. G. Wang and X. L. Xie provided invaluable assistance in the fieldwork. The personnel of the SHRIMP Center (D. Y. Liu, Y. R. Shi, and B. Song) helped us produce the zircon age data reported here. R. H. Zhang, G. S. Qiao, and Z. Y. Chu assisted in the Sr-Nd isotopic analyses. G. Q. He, J. Y. Li, D. H. Wang, and Y. C. Chen gave us very constructive comments. V. Kovach, I. Kozakov, and A. B. Kotov are thanked for their fruitful discussion and cooperation with research. We are grateful to an anonymous reviewer and W. J. Xiao for critical and helpful comments on this article. The work is supported by the Major State Basic Research Program of P. R. China (2001-CB409800), the National Natural Science Foundation of China (NSFC; grants 40472101, 40072023), the International Cooperation Project of the NSFC (grants 40211120647, 40472101), the China Geological Survey (grants 200113900018, 1212010611803), and the Foundation of the Key Laboratory of Northwest University, Xi'an, China. T. Wang is grateful for the financial support from the National Science Council (NSC; Taiwan), which allowed him to complete this work. B. Jahn acknowledges NSC grants (NSC93-2116-M-001-025, NSC94-2752-M-002-008-PAE, NSC94-2752-M-002-010-PAE) for the realization of this work.

REFERENCES CITED

Badarch, G.; Cunningham, W. D.; and Windley, B. F. 2002. A new terrane subdivision for Mongolia: implications for the Phanerozoic crustal growth of central Asia. J. Asian Earth Sci. 21:87–110.

Bau, M. 1996. Controls on the fractionation of isovalent trace elements in magmatic and aqueous systems: evidence from Y/Ho, Zr/Hf, and lanthanide tetrad effect. Contrib. Mineral. Petrol.123:323–333.

Black, L. P.; Kamo, S. L.; Williams, I. S.; Mundil, R.; Davis, D. W.; Korsch, R. J.; and Foudoulis, C. 2003. The application of SHRIMP to Phanerozoic geochronology; a critical appraisal of four zircon standards. Chem. Geol. 200:171–188.

Chappell, B. W., and White, A. J. R. 1992. I- and S-type granites in the Lachlan Fold Belt. Trans. R. Soc. Edinb. Earth Sci. 83:1–26.

Chen, B., and Jahn, B. M. 2002. Geochemical and isotopic studies of the sedimentary and granitic rocks of the Altai orogen of northwest China and their tectonic implications. Geol. Mag. 139:1–13.

Coleman, R. G. 1989. Continental growth of Northwest China. Tectonics 8:521–635.

Compston, W.; Williams, I. S.; Kirschvink, J. L.; Zhang, Z; and Guogan, M. 1992. Zircon U-Pb ages for the Early Cambrian timescale. J. Geol. Soc. Lond. 149: 171–184.

Elberg, M. A. 1996. Evidence of isotopic equilibration between microgranitoid enclaves and host grandiorite, Warburton Granodiorite, Lachlan Fold Belt, Australia. Lithos 38:1–22.

Gao, S.; Ling, W.; and Qiu, Y. 1999. Contrasting geochemical and Sm-Nd isotopic compositions of Archean metasediments from the Kongling high-grade terrain of the Yangtze craton: evidence for cratonic evolution and redistribution of REE during crustal anatexis. Geochim. Cosmochim. Acta 63:2071–2088.

Han, B. F., and He, G. Q. 1991. The tectonic nature of the Devonian volcanic belt of the southern margin of Altai Mountains, China. Geosci. Xinjiang 3:89–100 (in Chinese with English abstract).

He, G. Q.; Han, B. F.; Yue, Y. J.; and Wang, J. H. 1990. Tectonic division and crustal evolution of the Altai Orogenic Belt in China. Geosci. Xinjiang 2:9–20 (in Chinese with English abstract).

He, G. Q.; Li, M. S.; Liu, D. Q.; and Zhou, N. H. 1994. Palaeozoic crustal evolution and mineralization in

Xinjiang of China. Urumqi, Xinjiang People's Publishing House, 437 p.

Hu, A. Q.; Jahn, B. M.; Zhang, G. X.; Chen, Y. B.; and Zhang, Q. F. 2000. Crustal evolution and Phanerozoic crustal growth in northern Xinjiang: Nd isotopic evidence. Pt. I. Isotopic characteristics of basement rocks. Tectonophysics 328:15–51.

Hu, A. Q.; Wang, Z. G.; and Tu, G. Z. 1997. Geological evolution and metallogenetic regularity in northern Xinjiang. Beijing, Science Press, p. 52–62 (in Chinese).

Irber, W. 1999. The lanthanide tetrad effect and its correlation with K/Rb, Eu/Eu∗, Sr/Eu, Y/Ho, and Zr/Hf of evolving peraluminous granite suites. Geochim. Cosmochim. Acta 63:489–508.

Jahn, B. M.; Capdevila, R.; Liub, D.; Vernona, A.; and Badarch, G. 2004. Sources of Phanerozoic granitoids in the transect Bayanhongor-Ulaan Baatar, Mongolia: geochemical and Nd isotopic evidence, and implications for Phanerozoic crustal growth. J. Asian Earth Sci. 23:629–653.

Jahn, B. M.; Wu, F.; Capdevila, R.; Martineau, F.; Wang, Y.; and Zhao, Z. 2001. Highly evolved juvenile granites with tetrad REE patterns: the Woduhe and Baerzhe granites from the Great Xing'an (Khingan) Mountains in NE China. Lithos 59:171–198.

Jahn, B. M.; Wu, F. Y.; and Chen, B. 2000*a*. Granitoids of the Central Asian Orogenic Belt and continental growth in the Phanerozoic. Trans. R. Soc. Edinb. Earth Sci. 91:181–193.

———. 2000*b*. Massive granitoid generation in central Asia: Nd isotopic evidence and implication for continental growth in the Phanerozoic. Episodes 23:82–92.

Kovalenko, V. I.; Yarmolyuk, V. V.; Kovach, V. P.; Kotov, A. B.; Kozakov, I. K.; Sal'nikova, E. B.; and Larin, A. M. 2004. Isotope provinces, mechanisms of generation and sources of the continental crust in the Central Asian Mobile Belt: geological and isotopic evidence. J. Asian Earth Sci. 23:605–627.

Laurent-Charvet, S.; Charvet, J.; Monié, P.; and Shu, L. 2003. Late Paleozoic strike-slip shear zones in eastern central Asia (NW China): new structural and geochronological data. Tectonics 22:1009, doi:10.1029/2001TC901047.

Li, H. M.; Dong, S. W.; and Xu, J. S. 1995. Single zircon U-Pb dating of gabbros from Quanzhou: origin of basic magma in east Fujian province, China. China Sci. Bull. 40:158–160 (in Chinese).

Li, J. Y., Xiao; W. J.; Wang, K. Z.; Sun, G. H.; and Gao, L. M. 2003. Neoproterozoic-Paleozoic tectono stratigraphy, magmatic activities and tectonic evolution of eastern Xinjiang, NW China. *In*: Mao, J. W.; Goldfarb, R. J.; Seltman, R.; Wang, D. H.; Xiao, W. J.; and Hart, C., eds. Tectonic evolution and metallogeny of the Chinese Altay and Tianshan. International Association on the Genesis of Ore Deposits Guidebook Series 10. London, Centre for Russian and Central Asian Mineral Studies at the Natural History Museum, p. 31–74.

Liu, W. 1990. Ages and petrogenesis of granitoids in the Altai Mts., Xinjiang, China. Geotect. Metallogen. 14: 43–56 (in Chinese with English abstract).

———. 1993. Whole-rock isochron ages of plutons, crustal movements and evolution of tectonic setting in the Altai Mts., Xinjiang Uygur autonomous region. Geosci. Xinjiang 4:35–50 (in Chinese with English abstract).

Lou, F. 1997. Characteristics of late Caledonian granites in the Nuoerte area, Altay, China. Jiangxi Geol. 11: 60–66 (in Chinese with English abstract).

Ludwig, K. R. 1999. Isoplot/Ex, version 2.05: a geochronological toolkit for Microsoft Excel. Berkeley Geochronology Center Spec. Publ. 1a, p. 43.

Maniar, P. D., and Piccoli, P. M. 1989. Tectonic discrimination of granitoids. Geol. Soc. Am. Bull. 101:635–643.

Mei, H. J.; Yang, X. C.; Wang, J. D.; Yu, X. Y.; Liu, T. G.; and Bai, Z. H. 1993. Trace element geochemistry of late Paleozoic volcanic rocks on the southern side of the Irtysh River and the evolutionary history of tectonic setting. *In* Tu, G.Z., ed. Progress of solid earth sciences in northern Xinjiang, China. Beijing, Science Press, p. 199–216 (in Chinese).

Miller, R. B., and Paterson, S. R. 1994. The transition from magmatic to high-temperature solid-state deformation: implications from the Mount Stuart batholith, Washington. J. Struct. Geol. 16:853–865.

Paterson, S. R.; Fowler, T. K., Jr.; Schmidt, K. L.; Yoshinobu, A. S.; Yuan, E. S.; and Miller, R. B. 1998. Interpreting magmatic fabric patterns in plutons. Lithos 48:53–82.

Paterson, S. R.; Vernon, R. H.; and Tobisch, O. T. 1989. A review of the criteria for the identification of magmatic and tectonic foliations. J. Struct. Geol. 11:349–363.

Peccerillo, R.; and Taylor, S. R. 1976. Geochemistry of Eocene calc-alkaline volcanic rocks from the Kastamonu area, northern Turkey. Contrib. Mineral. Petrol. 76:58:63–81.

Qiao, G. S. 1988. Normalization of isotopic dilution analyses: a new program for isotope mass spectrometric analysis. Sci. Sin. (Ser. A) 31:1263–1268.

Rogers, G., and Hawkesworth, C. J. 1989. A geochemical traverse across the North Chilean Andes: evidence for crust generation from the mantle wedge. Earth Planet. Sci. Lett. 91:271–285.

Sajona, F. G.; Maury, R. C.; Bellon, H.; Cotten, J.; and Defant, M. 1996. High field strength element enrichment of Pliocene-Pleistocene island-arc basalts, Zamboanga Peninsula, western Mindanao (Philippines). J. Petrol. 37:693–726.

Sengor, A. M. C.; Natal'in, B. A.; and Burtman, V. S. 1993. Evolution of the Altaid tectonic collage and Paleozoic crustal growth in Eurasia. Nature 364:299–307.

Streckeisen, A., and Le Maitre, R. W. 1979. A chemical approximation to the modal QAPF classification of the igneous rocks. Neues Jahrb. Miner. Abh. 136:169–206.

Sun, S. S., and McDonough, W. F. 1989. Chemical and isotopic systematics of oceanic basalts: implications

for mantle composition and processes. *In* Saunders, A. D.; and Norry, M. J., eds. Magmatism in the ocean basins. Geol. Soc. Lond. Spec. Publ. 42:313–345.

Tong, Y.; Wang, T.; and Hong, D. W. 2005. Zircon U-Pb age of Tielike pluton in the western Altai orogen and its implications. Acta Geosci. Sin. 26:74–77 (in Chinese with English abstract).

Wang, T.; Zheng, Y. D.; Li, T. B.; and Gao, Y. J. 2004. Mesozoic granitic magmatism in extensional tectonics near the Mongolian border in China and its implications for crustal growth. J. Asian Earth Sci. 23: 715–729.

Wang, Z.; Sun, S.; Li, J.; Hou, Q.; Qin, K.; Xiao, W.; and Hao, J. 2003. Paleozoic tectonic evolution of northern Xinjiang, China: geochemical and geochronological constraints from the ophiolites. Tectonics vol. 22, doi: 10.1029/2002TC001396.

Wang, Z. G.; Zhao, Z. H.; and Zou, T. R. 1998. Geochemistry of the granitoids in Altay. Beijing, Science Press, p. 1–152 (in Chinese with English abstract).

Williams, I. S. 1998. U-Th-Pb geochronology by ion microprobe. Rev. Econ. Geol. 7:1–35.

Windley, B. F.; Kroner, A.; Guo, J. H.; Qu, G. S.; Li, Y. Y.; and Zhang, C. 2002. Neoproterozoic to Paleozoic geology of the Altai Orogen, NW China: new zircon age data and tectonic evolution. J. Geol. 110:719–737.

Wu, F. Y.; Jahn, B. M.; Wilde, S.; and Sun, D. Y. 2000. Phanerozoic crustal growth: U-Pb and Sr-Nd isotopic evidence from the granites in northeastern China. Tectonophysics 328:89–113.

Wu, F. Y.; Sun, D. Y.; Jahn, B. M.; and Wilde, S. 2004. A Jurassic garnet-bearing granitic pluton from NE China showing tetrad REE patterns. J. Asian Earth Sci. 23: 731–744.

Xiao, W. J.; Windley, B. F.; Badarch, G.; Sun, S.; Li, J.; Qin, K.; and Wang, Z. 2004. Palaeozoic accretionary and convergent tectonics of the southern Altaids: implications for the growth of central Asia. J. Geol. Soc. Lond. 161:339–342.

Xiao, X. C.; Tang, Y. Q.; Feng, Y. M.; Zhu, B. Q.; Li, J. Y.; and Zhao, M. 1992. Tectonic evolution of the northern Xinjiang and its adjacent region. Beijing, Geological Publishing House, pp. 1–180 (in Chinese, with English abstract).

Xu, J. F.; Castillo, P. R.; Chen, F. R.; Niu, H. C.; Yu, X. Y.; and Zheng, Z. P. 2003. Geochemistry of late Paleozoic mafic igneous rocks from the Kuerti area, Xinjiang, northwest China: implications for backarc mantle evolution. Chem. Geol. 193:137–154.

Xu, J. F.; Chen, F. R.; Yu, X. Y.; Niu, H. C.; and Zheng Z. P. 2001. Kuerti Ophiolite in Altay area of north Xinjiang: magmatism of an ancient back-arc basin. Acta Petrol. Mineral. 20:344–352 (in Chinese with English abstract).

Yang, J. H., and Zhou, X. H. 2001. Rb-Sr, Sm-Nd, and Pb isotope systematics of pyrite: implications for the age and genesis of lode gold deposits. Geology 29:711–14.

Zhang, H. X.; Niu, H. C.; Terada, K.; Yu, X. Y.; Sato, H.; and Ito, J. 2003. Zircon SHRIMP U-Pb dating on plagiogranite from Kuerti ophiolite in Altay, north Xinjiang. China Sci. Bull. 48:2231 2235.

Zhang, J. H., Wang, J. B.; and Ding, R. F. 2000. Characteristics and U-Pb ages of zircon in metavolcanics from the Kangbutiebao formation in the Altay orogen, Xinjiang. Reg. Geol. China 19:281–287.

Zhang, Q. F.; Hu, A. Q.; Zhang, G. X.; Cen, Y. B.; Nie, Y.; and Guo, D.Y. 1996*a*. Sm-Nd isochron age evidence for Precambrian metamorphic rocks from the eastern Junggar in northern Xinjiang, China. China Sci. Bull. 41:1896–1899.

Zhang, X. B.; Sui, J. X.; Li, Z. C.; Liu, W.; Yang, X. Y.; and Liu, S. S. 1996*b*. Study on tectonic evolution and mineralization series in the Eerqisi tectonic zone. Beijing, Science Press, p. 1–162 (in Chinese).

Zhang, Z. Q.; Lui, D. Y.; and Fu, G. M. 1994. Studies on the isotopic geochronology of the metamorphic stratum, North Qinling. Beijing, Geology Press, p. 21–76 (in Chinese with English abstract).

Zhao, Z. H.; Wang, Z. G.; Zou, T. R.; and Masuda, A. 1993. The REE, isotopic composition of O, Pb, Sr and Nd and petrogenesis of granitoids in the Altai region. *In:* Tu, G. Z. ed. Progress of solid-earth sciences in northern Xinjiang, China. Beijing, Science Press, p. 1–239 (in Chinese with English abstract).

Zou, T. R.; Cao, H. Z.; and Wu, B. Q. 1989. Orogenic and anorogenic granitoids of Altay Mountains of Xinjiang and their discrimination criteria. Acta Geol. Sin. 2: 45–64.